Multiple brain networks underpinning word learning from fluent speech revealed by independent component analysis

Diana López-Barroso[1,2,+], Pablo Ripollés[1,2,+], Josep Marco-Pallarés[1,2], Bahram Mohammadi[3,4], Thomas F.Münte[3], Anne-Catherine Bachoud-Lévi[5,6], Antoni Rodriguez-Fornells[1,2,7], Ruth de Diego-Balaguer[1,2,6,7]

[1]Cognition and Brain Plasticity Unit. Bellvitge Research Biomedical Institute (IDIBELL), Hospitalet de Llobregat, 08907 Barcelona, Spain

[2]Dept. of Basic Psychology, University of Barcelona, 08035 Barcelona, Spain

[3]Department of Neurology, University of Lübeck, Lübeck, Germany

[4]CNS-LAB, International Neuroscience Institute (INI), Hannover, Germany

[5] INSERM U955, Equipe 1, Neuropsychologie Interventionnelle, IMRB, Créteil, France

[6] Ecole Normale Superieure, Departement d'Etudes Cognitives, Paris, France

[7] Institució Catalana de Recerca i Estudis Avançats (ICREA), Barcelona, Spain

[+]Diana López-Barroso and Pablo Ripollés contributed equally to the present study

Corresponding author: Diana López-Barroso

University of Barcelona

Faculty of Psychology

Department of Basic Psychology

Pg. Valld'Hebron 171

08035 Barcelona (Spain)

Abstract

The contribution of the different brain networks to word learning from fluent speech is still largely unknown, although neuroimaging studies using standard subtraction-based analysis have suggested that frontal and temporal regions are involved in it. However, this type of analysis cannot identify the extent of distributed networks that are engaged by a complex task such as word learning. Here we use Independent Component Analysis (ICA) – a multivariate approach – to characterize the different brain networks subserving word learning from an artificial language speech stream containing novel words. Four spatially independent networks were associated with the task: (i) a dorsal Auditory-Premotor network; (ii) a dorsal Sensory-Motor network; (iii) a dorsal Fronto-Parietal network; and (iv) a ventral Fronto-Temporal network. A further, fine-grained analysis of the network level of engagement across time showed that the engagement of these networks varied through the learning period with only the network covering auditory and motor areas being engaged across all blocks. In addition, the connectivity strength of this network in the first and second blocks correlated with the individual variability in word learning performance. These findings obtained with a data-driven approach suggest that: (i) word learning relies on segregated connectivity patterns involving dorsal and ventral networks; and (ii) specifically, the dorsal auditory-premotor network connectivity strength is directly correlated with word learning performance.

Keywords: dorsal-stream, ventral stream, word-learning, functional connectivity, ICA.

Despite the apparent ease with which humans speak and communicate, learning a new language is a complex task which everyone needs to face at least once in her or his lifetime. A central aspect of this process is the acquisition of new words. In natural circumstances, learners need to first discover word units from fluent speech. This process may rely on statistic-based mechanisms which track regularities between phonemes and syllables as well as on the detection of the subtle prosodic cues that can help word segmentation (e. g. pauses, intonation, etc.; Aslin et al., 1998; Peña et al., 2002). Then, memory traces of those isolated word forms need to be progressively enhanced through subsequent encounters (Saffran, 2001) in order to be memorised and stored in long-term memory (for a review: Rodriguez-Fornells et al., 2009).

Therefore, like for other complex cognitive functions, learning of new words may rely on widespread segregated and overlapping large-scale networks (Mesulam, 1990), even before meaning is attached to them. Interestingly, we have recently shown that the ability to learn novel word forms is related to functional and structural connectivity between the auditory cortical area (comprising the superior temporal gyrus, STG) and the motor regions (comprising the premotor cortex, PMC; and the inferior frontal gyrus, IFG) through the direct connection of the arcuate fasciculus in the left hemisphere (López-Barroso et al., 2013). These regions belong to the dorsal stream of language processing, which is in charge of mapping sound into articulation (Hickok and Poeppel, 2000; Hickok et al., 2011; Rauschecker and Scott, 2009; Saur et al., 2008), a process that might be involved in the acquisition of new vocabulary (Hickok and Poeppel, 2007; Rodriguez-Fornells et al., 2009). At the same time, the areas of the dorsal stream along with the

inferior parietal lobe (Buchsbaum and D'Esposito, 2008; Corbetta and Shulman, 2002) are related to the rehearsal and attentional mechanisms necessary to maintain phonological information in working memory (Jacquemot and Scott, 2006); a function that is likely to be required to keep the phonological form of the segmented word in an active state in order to be memorized.

Thus far, previous reports of functional neuroimaging of the very first stages of word learning are limited (Cunillera et al., 2009; Karuza et al., 2013; McNealy et al., 2011, 2006). Despite of some methodological differences, all of these studies required participants to listen to a continuous flow of speech composed of nonsense trisyllabic words with no meaning attached. McNealy et al. (2006) identified increased activity in the left inferior and middle frontal gyrus when comparing words (presented during the learning phase) with partwords as the neural signature of on-line word learning. In addition, during learning, temporal and parietal regions showed increased activity when listening to a stream containing words compared to a stream containing syllables in random order. Cunillera et al. (2009) also reported the involvement of the PMC during the initial stages of the learning process. Finally, a recent study reported a correlation between IFG activation and the implicit capacity to segment words (Karuza et al., 2013). Although the univariate analysis approach taken by these studies only allows to spot the involvement of a variety of independent regions, the regions highlighted suggest an involvement of the dorsal stream in word learning. However, to date there is no information about how these segregated regions functionally interact during word learning.

Here we used independent component analysis (ICA) to identify the whole set of functional networks engaged during a word-learning task. ICA is a data-driven approach (Calhoun et al., 2008) that allows the measurement of both the BOLD response fluctuations in the active brain and the spontaneous fluctuations in the resting brain (Smith et al., 2009), capturing the integrated activity of spatially distributed brain regions (i.e. functional integration; Friston, 2011; Smith, 2012) without any a priori constraint. ICA is especially well-suited to discern how multiple functional networks — subserving different cognitive processes — synergistically interact (Calhoun et al., 2001; Celone et al., 2006; Wu et al., 2009). ICA presents some advantages over univariate analysis. For example, it does not need a temporal model of brain functioning. Univariate analysis provides optimal results when the activated areas follow a close to canonical BOLD response, but in contrast, is blind to other types of changes (for example transient task-related, non-task related, slow varying, etc., Calhoun et al., 2009; McKeown et al., 1998). Moreover, recent studies have shown that different neural circuits can occur concurrently within the same brain areas, but cannot be resolved by standard GLM analysis (Beldzik et al., 2013; Xu et al., 2013a, 2013b).

In this study, participants completed an artificial word-learning task which tapped the initial stages of word learning, when auditory word forms need to be learned from fluent speech and no meaning is yet associated to them (De Diego-Balaguer et al., 2007; Peña et al., 2002). First, we aimed to define the brain networks that are engaged and disengaged during the word-learning task. As the ICA analysis is fully data-driven, similar experiments were performed in two different samples of participants with different linguistic backgrounds (Spanish

[n=25] and German [n=16]), searching for replication (Bennet et al., 2009; Button et al., 2013; Lieberman and Cunningham, 2009). Second, we aimed to study which of the engaged networks is associated with the individual variability in the word learning performance.

Material and Methods

Participants

Forty-three participants were recruited for the study. Twenty-seven native Spanish speakers (mean age: 24.7, SD: 4.6, 12 women) were involved in the main study. The second cohort involved sixteen volunteers (mean age, 26.6; SD: 4.6, 8 women) that were studied for replication purposes. Participants from the second cohort were all native German speakers. Written consent was obtained from all subjects and they were paid for their participation. They all were free of neurological and otological diseases and had no history of auditory problems. Both experiments were approved by the respective local ethical committees.

Artificial Word-Learning Task

First cohort. The experiment involved a learning and a test phase. During the learning phase, subjects conducted an artificial word-learning task administered in two runs. Eight different artificial languages were used, including six that had been employed in a previous study (De Diego-Balaguer et al., 2007) and two new languages that had been validated in a behavioural pilot study. Stimuli were

presented through MR-compatible headphones. Each participant heard two of the eight languages created, one in each run. The order of the languages was counterbalanced among subjects. Streams and test items were built using MBROLA speech synthesizer software (Dutoit et al., 1996). The languages were built by concatenating nine different trisyllabic nonsense words (De Diego-Balaguer et al., 2007; Peña et al., 2002; Saffran et al., 1996) that followed Spanish phonotactic constraints. Words had a duration of 696 ms each, and subtle pauses of 25 ms were inserted between them in order to introduce a prosodic cue to enhance the segmentation process. During the task, 4 active blocks, each including 42-word presentations (30 seconds), were alternated with resting blocks of 20 seconds duration. Words were presented in the form of a fluent speech stream and concatenated pseudo-randomly such that the same word was never immediately repeated in the stream. Participants were told to pay attention to the nonsense language stream, as later on they would be asked about "words" presented within the streams.

After the language exposure in each run, word learning was assessed behaviorally by testing words that had been presented during the learning phase and words that had not been presented and that did not conform to the rules of the language ("non-words"). Non-words were built with the same syllables as real words, but in an incorrect order. Responses were recorded using an MR-compatible response box containing two response buttons (forefinger and middle-finger of the left hand). Participants heard a word or non-word presented in isolation and they were required to press with the middle finger button if they thought that it had been presented as a word of the learned language and with the

index finger if they thought that it was a non-word. The experiment was presented using the Presentation Software. In order to assess participants' ability to correctly discriminate words from non-words, their behavioural responses were transformed into d-prime scores (MacMillan and Creelman, 2005). The subjects' overall performance indicated that words of the languages were indeed learned (behavioural data for two subjects was not available due to technical problems in the recording): participants reliably distinguished between words and non-words ($t(24) = 2.74$, $p < 0.01$).

Second cohort. For the second cohort, given that participants were native German speakers, the materials were modified to use German phonemes. This was done by applying the German diphone database from the MBROLA text-to-speech synthesizer. Speech streams preserved German phonotactics. The same procedure as for the main experiment was used for the learning and test phases except that, in order to have a greater signal-to-noise relation, 3 runs with 6 language-rest blocks per run were used. The duration of each active and resting block was the same as for the main experiment. Although responses could not be recorded in this scanner, to maintain the same procedure as in the main experiment, participants were required to respond during the test phase in the same manner as the participants from the first cohort. The materials used were tested in another group of participants (N=13) and confirmed that learning was also possible with the modified version of the material ($t(12) = 4.27$, $p < 0.001$).

Image Acquisition

First Cohort. Images were acquired using a 3.0 Tesla Siemens Trio MRI system at the Hospital Clinic of Barcelona. Functional images were obtained using a single-shot T2*-weighted gradient-echo EPI sequence (slice thickness = 4mm; no gap; number of slices = 32, order of acquisition interleaved; repetition time (TR) = 2000 ms; echo time (TE) = 29 ms; flip angle = 80º; matrix = 128 x 128; field of view FOV = 240 mm; voxel size = 1.87x1.87x4 mm^3). Each slice was aligned to the plane intersecting the anterior and posterior commissures. In addition to the functional runs a high-resolution T1-weighted image (slice thickness = 1mm; no gap; number of slices = 240; repetition time (TR) = 2300ms; echo time (TE) = 3ms; matrix = 256 x 256; field of view (FOV) = 244 mm) was also acquired for each subject.

Second cohort. Images were acquired using a 3.0 Tesla Siemens Allegra MRI system at International Neuroscience Institute in Hannover, Germany. Functional images were obtained using a single-shot T2*-weighted gradient-echo EPI sequence (slice thickness = 3 mm; distance factor = 25% (0,7 mm); number of slices = 34, order of acquisition interleaved; repetition time (TR) = 2000 ms; echo time (TE) = 30ms; flip angle = 80º; matrix = 128 x 128; FOV = 192 mm; voxel size = 3x3x3 mm^3). Each slice was aligned to the plane intersecting the anterior and posterior commissures. In addition to the functional runs a high-resolution T1-weighted image (slice thickness = 1mm; no gap; number of slices = 192; repetition time (TR) = 15 ms; echo time (TE) = 4.9 ms; matrix = 256 x 256; FOV = 256 mm) was also acquired for each subject.

Preprocessing and ICA analysis

The ICA analysis was performed on the fMRI data from the learning phase of the experiment. Data were preprocessed using Statistical Parameter Mapping software (SPM8, Wellcome Department of Imaging Neuroscience, University College, London, UK, www.fil.ion.ucl.ac.uk/spm/). For the main experiment`, the two functional runs were realigned and their mean image was calculated. The structural T1s were co-registered to their respective mean functional image and segmented using the New Segment toolbox included with SPM8. Following segmentation, grey and white matter images were fed to DARTEL (Ashburner, 2007) in order to achieve normalization. After normalization, data was subsampled to 1.5x1.5x1.5 mm^3 (121x145x121 voxels) and spatially smoothed with an 8x8x8 full width at half maximum (FWHM) Gaussian kernel. For the second cohort of subjects (replication study), the three functional runs were also realigned and a mean image of all the EPIs was created. After an initial 12-parameter affine transformation of this mean to the EPI MNI template, the resulting normalization parameters derived were applied to the whole functional set. Finally, functional EPI volumes were re-sampled into 4x4x4 mm voxels and spatially smoothed with an 8 mm FWHM kernel.

Group Spatial ICA was used to extract the different networks present during each of the experiments using the GIFT software (http://icatb.sourceforge.net/). ICA was applied with the number of independent components set to 20, which has been shown to be an optimal dimension in previous studies (Forn et al., 2013; Smith et al., 2009). Following this, the functional images from each of the experiments were analyzed using group ICA, which started with an intensity

normalization step. After this first step, data was first concatenated and then reduced to 20 temporal dimensions (using principal component analysis), to be then analysed with the infomax algorithm (Bell and Sejnowski, 1995). No scaling was used, as with the intensity normalization step, the intensities of the spatial maps obtained are already in percentage of signal change.

A one-sample t-test was calculated using the individual spatial maps, which treats each subject's network as a random effect (Calhoun et al., 2001). All networks (see Figure 2) are shown at $p < 0.01$ corrected using false discovery rate (FDR) algorithm with a cluster extent of 30 voxels. FDR correction has been widely used to report ICA components (Calhoun et al., 2008, 2001; Eichele et al., 2008; Forn et al., 2013; Wu et al., 2009).

Calculation of task-related networks

In order to identify which of the networks retrieved were related to task (i. e., word learning from fluent speech), a multiple regression was calculated using GIFT. This allows fitting each subject's component time course to the model. Models were created using SPM8 by convolving a canonical hemodynamic response with the timing of the active and resting blocks of the word-learning task. First, a model including only two conditions was created: learning from fluent speech and rest. A one-sample t-test was performed on all the beta values obtained from the learning condition regressor for each of the extracted networks. A network was considered task-related if the regressor survived the fit ($p < 0.05$; Calhoun et al., 2008; Forn et al., 2013; see Figure 2 and Tables 3 and 4). The

analysis of the task-relatedness of the networks extracted for the second cohort was done specifically to replicate the results obtained from the first. Independent replication is crucial to differentiate true effects from random noise and to firmly establish a result (Bennet et al., 2009; Button et al., 2013). It also minimizes Type I errors, as false positives are not likely to replicate across different studies (Lieberman and Cunningham, 2009). At the same time it allows avoiding committing Type II errors that may rise from a too restrictive Bonferroni correction. Replicating the same networks in two different cohorts of individuals with different language backgrounds, with MRI data being collected in different scanners, and also using two different sets of stimuli (one following the phonotactic rules of Spanish and the other of German) provides compelling prove that the reported networks do not come from spurious correlations. Consider for instance this, we took advantage of our replication study and we focus our discussion on the networks that are significantly engaged during both the main experiment and the replication experiment.. However, our strongest claims are based in the networks that also survived the correction for multiple comparisons. (see Result section). Indeed, Tables shows which of the task-related networks survived a Bonferroni correction (p-values under 0.0025 survived the correction for multiple comparisons, as 20 networks were tested).

Relationship between network engagement and learning performance

Once the networks significantly engaged during word learning were established, a second fine-grained task-related analysis was performed. The aim

was to relate each task-related network with learning performance over time, we calculated a new model defining 5 conditions: learning from fluent speech during block 1, 2, 3 and 4, and rest. This analysis was only performed for the first cohort of participants (main experiment), as behavioural responses inside the scanner were not available for the second cohort (replication study). Therefore, an independent beta value for each of the four blocks comprising the task was extracted for the 5 task-related networks replicated in both studies. Once again, a one-sample t-test was carried out on all the beta values for the active task regressor of each block ($p < 0.05$). The networks surviving the correction for multiple comparisons are indicated in Table 5 (p-values under 0.0025, as four blocks were tested for 5 networks). Finally, Pearson's correlation analysis was performed between word learning performance (d prime) and each participant's beta value only for the blocks and networks that survived the correction. No correction for multiple comparisons was applied in this last correlation analysis that was focused only in the significant blocks (4 blocks from the dAPMN, and 2 blocks from the dSMN, See Results section) to confirm their direct relationship with learning performance.

Results

ICA decomposition

First cohort. Three out of the 20 ICA networks retrieved were significantly positively correlated to the word-learning task (see Table 1 for statistical values) with a fourth one being marginally related ($p = 0.052$). These same three networks were also retrieved as task-related in the second cohort of subjects, replicating this

result (see below). From those, only two out of three networks survived the correction for multiple comparisons (Table 1). The task-related ICA maps (networks) are displayed in Figure 2 (left panels) along with their respective BOLD time courses. Three of these networks were considered "dorsal" networks (Table 1): a dorsal *Auditory-Premotor Network* (dAPMN, Figure 2A) covering the bilateral superior temporal gyrus (STG) and superior temporal sulcus (STS) extending to the dorsal part of the middle temporal gyrus (MTG), the Sylvian Parietal Temporal area (SPT), the premotor cortex (PMC), the supplementary motor area (SMA) and pre-SMA; a dorsal *Sensory-Motor Network* (dSMN, Figure 2B) comprising the pre- and post-central gyri, PMC and SMA; and a left lateralized dorsal *Fronto-Parietal Network* (dFPN, Figure 2C) covering mainly frontal (including the inferior [IFG] and middle [MFG] frontal gyrus) and parietal (both inferior and superior) areas. Both the dAPMN and dSMN networks survived Bonferroni correction. The fourth network, marginally related to the task, was identified as a ventral *Fronto-Temporal Network* (vFTN, Figure 2D), covering the prefrontal and insular cortex, the anterior superior and middle temporal cortex and the caudate nucleus. Finally, the *Default Mode Network* (DMN, Figure 3A) was the only network significantly negatively correlated with the task. The DMN comprised its typical constituents, i.e. bilateral parietal and occipital gyri, the precuneus, posterior and middle cingulate gyri, the superior middle frontal and the anterior cingulate gyri.

The remaining 15 networks that did not pass the threshold to be considered related to the task ($p < 0.05$) were visually inspected in order to detect artifactual components reflecting movements, ventricles, edges or the presence of blood vessels, and 8 were discarded. The other 7 networks were labelled as: *Superior*

Parietal, *Lateral Visual*, *Cerebellar*, *Medial Visual*, *Cingulate*, *Mesial Temporal* and right *Fronto*-Parietal (see Table 3). All of these networks have been previously identified and reported both during active task and resting state paradigms (Forn et al., 2013; Smith et al., 2009; Tie et al., 2008).

Second cohort. Six out of the 20 ICA networks retrieved were significantly positively correlated to the word-learning task (see Table 2 for statistical values). The three task-related networks identified in the first cohort (dAPMN, dSMN, dFPN) were among those six networks. In addition, it is worth mentioning that the fourth network, the vFTN, passed the significance threshold ($p < 0.045$, see Table 2 and Figure 2, right panel) while in the main experiment this network resulted marginally related ($p = 0.052$). Importantly, the areas belonging to these networks were highly consistent compared with the ones belonging to the networks from the first experiment (see Figure 2, left panel). As in the first cohort, the dAPMN and dSMN engagement survived multiple comparison correction. The two other networks that correlated with the model were an *Insular Network* comprising the insula bilaterally and the SMA; and a *Lateral Visual Network* covering the lateral aspects of bilateral superior, middle and inferior occipital and fusiform gyri (Table 2). The latter network was retrieved also in the first cohort but did not appear related to the task (see Table 3 for statistical values). Again, the DMN was the only network significantly negatively correlated with the task (see Figure 3B). From the other 13 networks not related to the task, six were considered artifactual and the remaining 7 networks were very similar to the task-independent networks of the first cohort. These networks have also been previously reported both in task-

related and resting state ICA studies (Forn et al., 2013; Smith et al., 2009; Tie et al., 2008) and were labelled as *Medial Visual*, *Medial Inferior Visual* (covering mainly the calcarine visual cortex), *Cerebellar*, *Mesial Temporal*, right *Fronto-Parietal*, *Posterior DMN* and *Superior Medial Fronto-Parietal* (see Table 4 for a description and statistical analysis).

Network engagements across blocks and word learning performance

First Block: the dAPMN, the dSMN, the dFPN and the vFPN were active during the first block, while the DMN was deactivated (Table 5 and Figure 4). *Second block*: only the dAPMN remained significantly active, while the DMN was again significantly disengaged (Table 5 and Figure 4). *Third block*: only the dAPMN was active during the third block (Table 5 and Figure 4). *Fourth block:* the dAPMN and the dSMN were active during the last block (Table 5 and Figure 4). The dAPMN engagement survived Bonferroni correction in all blocks and the dSMN in the first and fourth blocks.

Correlation analyses revealed that the strength of connectivity of the dAPMN during the second block was significantly correlated with word learning performance ($r = 0.40$, $p < 0.047$; Figure 5). A positive trend was also found during the first block although the p value did not reach the threshold for significance ($r = 0.34$, $p = 0.08$; Figure 5).

Discussion

In this study we identified several brain networks whose connectivity strength increases when adult participants are learning words from fluent speech. While being exposed to a novel language, three networks were engaged in two different and independent samples of subjects, and a fourth one was significant for one sample and marginal for the other. Following previous language processing models (Hickok and Poeppel, 2007; Rauschecker and Scott, 2009), the three networks were classified as dorsal language related networks. Specifically, an auditory-premotor network, a sensory-motor network (dSMN) and a fronto-parietal network (dFPN; see Figure 2A, B and C) were identified. Thus, segregated sub-networks within the dorsal stream contribute differentially to the word learning process. Of these, the dAPMN was significantly active during all four blocks, while the dSMN was active during the first and last block (Figure 4). The fourth task-related network, part of the ventral stream of speech processing, was also found (vFTN; see Figure 2D). The dFPN and the ventral network showed a trend to be active only during the first block. Expectedly, the default mode network showed an opposite pattern, as it was negatively correlated with the task. In addition, the block-wise analysis showed that this network is significantly disengaged during the early presentation of the stimuli, but does not show a negative correlation during the last two blocks (Figure 4). Interestingly, only the variability in the dAPMN directly correlated with the differences in individual learning performance during the second block of the task (and marginally during the first one; Figure 5). These results suggest that connectivity between motor and auditory areas is important in the very early stages of learning when word forms are extracted from fluent speech. Importantly our results were obtained through Independent

Component Analysis, a fully data-driven approach without any a priori assumption. Although these networks have been reported elsewhere during resting state (e.g. Beckmann et al., 2005; Smith et al., 2009), here we report their specific contribution to word learning.

The implication of the five reported networks in word learning was supported by the fact that our results were replicated in a second cohort of subjects. Virtually identical task-related networks were observed across both studies, in spite of different linguistic backgrounds (Spanish vs. German learners with Spanish and German phonemes respectively), variable MRI technology (two different 3T scanners) and acquisition parameters (see Material and Methods section). This further backs our claim as false positives are not likely to replicate across independent samples (Bennet et al., 2009; Button et al., 2013; Lieberman and Cunningham, 2009).

Dorsal networks for word learning

We found three networks that belong to the dorsal fronto-temporo-parietal stream of language processing (Hickok and Poeppel, 2000; Saur et al., 2008). First, the dorsal *Auditory-Premotor Network* (Figure 2A), connecting the pSTG (including the Spt region, located within the Sylvian fissure at the parieto-temporal boundary), the PMC and the bilateral SMA, has been associated with auditory-motor integration (Hickok and Poeppel, 2000; Liberman and Whalen, 2000), an inherent mechanism of language processing. Interestingly, in our study this was the only network (i) that was significantly engaged during the four blocks; (ii) that showed the most robust engagement, as it did survive multiple comparisons

corrections in the different analyses and (iii) whose connectivity strength during the second block of the learning phase (and marginally during the first) was directly correlated with word learning. These two properties fit well with a recent study in which we reported the importance of the direct left segment of the arcuate fasciculus for word learning and the functional connectivity between the areas connected by this fascicle (López-Barroso et al., 2013). In this previous study nevertheless, the analyses were restricted to the areas of theoretical interest and therefore whole brain connectivity was not assessed. The consistent finding in this different study with an additional replication in a cohort from a different language background and with a data-driven approach gives further strength to the results.

The importance of motor regions for language processes is also supported by the implication of the PMC in speech perception (Meister et al., 2007; Pulvermüller et al., 2006; Wilson and Iacoboni, 2006). Also, Rauschecker and Scott (2009) proposed a unified function of the dorsal stream in which the PMC informs the auditory system about the planned motor sequences that are about to happen (overtly or covertly), and this is matched with feedback signals from auditory areas (pSTG), closing the loop. The template-matching function of this network can therefore have a particularly important role during word learning from speech (Rodriguez-Fornells et al., 2009). Our results suggest that this function is particularly important during the initial contact with the new language, when word forms need first to be extracted, to be then kept in working memory and memorized.

Second, sensory and motor regions were also engaged during the task, as supported by the identification of the dorsal *Sensory-Motor Network* (dSMN, Figure

2B). Primary related to motor functions (Biswal et al., 1995), this bilateral network comprises regions from the precentral and postcentral gyri in addition to supplementary and pre-supplementary motor and cingulate areas. These regions have been related to speech production (Alario et al., 2006; Chauvel et al., 1996; Crosson et al., 2001; Krainik et al., 2004; Ziegler et al., 1997). Although its exact role is still unclear, the anterior part of the SMA is reliably involved in sequence learning (Hikosaka et al., 1996; Penhune and Steele, 2012). This network was significantly engaged during the first and the last blocks of learning, suggesting that the planning of the articulatory movements (Lau et al., 2004) required for the covert rehearsal (López-Barroso et al., 2011) occurs to a greater extent during the early contact with the new language for the sequences of syllables (first block) and then in the last block when word chunks are already segmented and rehearsed for memorisation.

Third, a left dorsal *Fronto-Parietal Network* (dFPN, Figure 2C) comprising the inferior and superior parietal cortex, the IFG, the dorsolateral prefrontal gyrus and the PMC was identified, which might be considered as the classical language network. The inferior parietal lobe has been previously identified as an important region in vocabulary learning and second-language learning (Golestani and Pallier, 2007; Leh et al., 2007; Mechelli et al., 2004). This whole network overlaps with the attentional network (Corbetta and Shulman, 2002; Salmi et al., 2009) and includes the supramarginal gyrus (SMG), involved also in the maintenance of phonological information in working memory through an attentional controller mechanism or through short-term storage (Awh et al., 1996; Chein et al., 2003; Cowan, 2008; Ravizza et al., 2004). The appearance of this network suggests an engagement of both

working memory and attention functions in learning of phonological word forms (Baddeley, 2003; De Diego-Balaguer and Lopez-Barroso, 2010; López-Barroso et al., 2011; Rodriguez-Fornells et al., 2009).

Ventral network for word learning

The ICA analysis also revealed a ventral *Fronto-Temporal* network (Figure 2D), which comprises the bilateral anterior temporal areas, the IFG area (including the frontal operculum [FOP]) as well as the bilateral striatum. Although classically associated to conceptual-semantic analysis (Binder et al., 2009; Hickok and Poeppel, 2007; Lambon Ralph et al., 2012; Patterson et al., 2007), the implication of the ventral network in auditory object recognition has been also proposed, allowing categorization of the incoming auditory stimulation as new or familiar (Leaver and Rauschecker, 2010; Rauschecker and Scott, 2009; Zatorre et al., 2004). In agreement with this, and regarding the task used in the current study, the ventral stream could have a role in the recognition of the phonological chunks (new words) once they have been segmented. Its engagement during word form learning even when there is no semantic component agrees with previous results indicating a prominent role of this ventral stream when support to the dorsal stream is needed (López-Barroso et al., 2011; Saur et al., 2010). In addition, the caudate nucleus forms part of this network, which agrees with the importance of this area for the concatenation of sequences forming a chunk (Koechlin and Jubault, 2006) in artificial language learning from visual or auditory sequences

(Bahlmann et al., 2008; De Diego-Balaguer et al., 2008; Doeller et al., 2006; Lieberman, 2000).

Interestingly, the four networks identified in the study seem to be organized in a caudal-dorsal to rostral-ventral fashion (see Figure 6). This organization fits well with studies proposing a hierarchical functional organization of the lateral frontal cortex in relation to cognitive control. Applied to sequential linguistic processing (e.g. phonemes, syllables, words in sentences) this could mean that rostral (anterior) regions control more abstract and complex structures and caudal (posterior) regions process and control more concrete information (Badre and D'Esposito, 2009; Bahlmann et al., 2014, 2012; Christoff et al., 2009; Koechlin and Jubault, 2006).

The Default Mode Network

The *Default Mode Network (DMN);* see Figure 3) was negatively correlated with the task. This finding is consistent with the characteristics of the DMN. Since it was first described (Raichle et al., 2001), the DMN has been related to the gathering of incoming sensory information at rest and has been reported as deactivated during active tasks (Kuperberg et al., 2003; Mestres-Missé et al., 2008; Smith et al., 2009). The block-wise analysis showed that the DMN was disengaged during the first two blocks of stimulation. The concomitant correlation in these blocks with learning performance for the dAPMN may indicate that as learning increases, the DMN gradually engages since the task progressively becomes less demanding.

Finally, it is worth mentioning that in spite of the advantatges of using ICA to unveil unconstrained brain connectivity compared to classical GLM fMRI analysis, this study has also limitations that should be faced in future investigation. Specifically, while ICA assesses functional connectivity, the interactions between networks are not uncovered. Further studies are needed in order to assess the direct influence and direction of the coupling that each network (or nodes within these networks) exerts over other the nodes (i.e., effective connectivity).

Acknowledgments

This research has been supported by a predoctoral grant from Generalitat de Catalunya to DLB (2010FI B1 00169), the Spanish Government FPU program (AP2010-4179) to PR and the Ramon y Cajal programme awarded to JMP. RDB has been supported by FP7 ERC StG_313841 TuningLang. ARF and RDB have been supported by grants from the Spanish Government (MICINN, PSI2011-29219 to ARF/PSI2011-23624 to RDB) and the Catalan Government (Generalitat de Catalunya, 2009 SGR 93). TFM has been supported by the DFG and BMBF and ACBL has been supported by a "Contrat interface" INSERM.

References

Alario, F.-X., Chainay, H., Lehericy, S., Cohen, L., 2006. The role of the supplementary motor area (SMA) in word production. Brain Res 1076, 129–43.

Ashburner, J., 2007. A fast diffeomorphic image registration algorithm. Neuroimage 38, 95–113.

Aslin, R.N., Saffran, J.R., Newport, E.L., 1998. Computation of conditional probability statistics by 8-month-old infants. Psychological Science 9, 321–324.

Awh, E., Jonides, J., Smith, E.E., Schumacher, E.H., Koeppe, R.A., Katz, S., 1996. Dissociation of storage and rehearsal in verbal working memory: Evidence From Positron Emission Tomography. Psychol Sci 7, 25–31.

Baddeley, A., 2003. Working memory and language: an overview. Journal of Communication Disorders 36, 189–208.

Badre, D., D'Esposito, M., 2009. Is the rostro-caudal axis of the frontal lobe hierarchical? Nat Rev Neurosci 10, 659–69.

Bahlmann, J., Blumenfeld, R.S., D'Esposito, M., 2014. The Rostro-Caudal Axis of Frontal Cortex Is Sensitive to the Domain of Stimulus Information. Cerebral cortex.

Bahlmann, J., Korb, F.M., Gratton, C., Friederici, A.D., 2012. Levels of integration in cognitive control and sequence processing in the prefrontal corte. PLoS One 7.

Bahlmann, J., Schubotz, R.I., Friederici, A.D., 2008. Hierarchical artificial grammar processing engages Broca's area. Neuroimage 42, 525–34.

Beckmann, C.F., DeLuca, M., Devlin, J.T., Smith, S.M., 2005. Investigations into resting-state connectivity using independent component analysis. Philos Trans R Soc Lond B Biol Sci 360, 1001–1013.

Beldzik, E., Domagalik, A., Daselaar, S., Fafrowicz, M., Froncisz, W., Oginska, H., Marek, T., 2013. Contributive sources analysis: a measure of neural networks' contribution to brain activations. Neuroimage 76, 304–312.

Bell, a J., Sejnowski, T.J., 1995. An information-maximization approach to blind separation and blind deconvolution. Neural Comput 7, 1129–59.

Bennet, C.M., Wolford, G.L., Miller, M.B., 2009. The principled control of false positives in neuroimaging. Soc. Cogn. Affect. Neurosci. 4, 417–422.

Binder, J.R., Desai, R.H., Graves, W.W., Conant, L.L., 2009. Where is the semantic system? A critical review and meta-analysis of 120 functional neuroimaging studies. Cereb Cortex 19, 2767–2796.

Biswal, B., Yetkin, F.Z., Haughton, V.M., Hyde, J.S., 1995. Functional connectivity Echo-Planar MRI. Magn Reson Med 34, 537–541.

Buchsbaum, B.R., D'Esposito, M., 2008. The search for the phonological store: from loop to convolution. J Cogn Neurosci 20, 762–78.

Button, K.S., Ioannidis, J.P., Mokrysz, C., Nosek, B.A., Flint, J., Robinson, E.S., Munafo, M.R., 2013. Power failure: why small sample size undermines the reliability of neuroscience. Nat Rev Neurosci 14, 365–376.

Calhoun, V., Kiehl, K., Pearlson, G., 2008. Modulation of temporally coherent brain networks estimated using ICA at rest and during cognitive tasks. Hum Brain Mapp 29, 828–838.

Calhoun, V.D., Adali, T., Pearlson, G.D., Pekar, J.J., 2001. A Method for Making Group Inferences from Functional MRI Data Using Independent Component Analysis. Hum Brain Mapp 14, 140–151.

Calhoun, V.D., Liu, J., Adali, T., 2009. A review of group ICA for fMRI data and ICA for joint inference of imaging, genetic, and ERP data. Neuroimage 45, S163–S172.

Celone, K. a, Calhoun, V.D., Dickerson, B.C., Atri, A., Chua, E.F., Miller, S.L., DePeau, K., Rentz, D.M., Selkoe, D.J., Blacker, D., Albert, M.S., Sperling, R. a, 2006. Alterations in memory networks in mild cognitive impairment and Alzheimer's disease: an independent component analysis. J Neurosci 26, 10222–31.

Chauvel, P., Rey, M., Buser, P., Bancaud, J., 1996. What stimulation of the supplementary motor area in humans tells about its functional organization. Adv Neurol 70, 199–209.

Chein, J.., Ravizza, S.., Fiez, J.., 2003. Using neuroimaging to evaluate models of working memory and their implications for language processing. J Neuroling 16, 315–339.

Christoff, K., Keramatian, K., Gordon, A.M., Smith, R., Mädler, B., 2009. Prefrontal organization of cognitive control according to levels of abstraction. Brain Res 1286, 94–105.

Corbetta, M., Shulman, G.L., 2002. Control of goal-directed and stimulus-driven attention in the brain. Nat Rev Neurosci 3, 201–215.

Cowan, N., 2008. What are the differences between long-term, short-term, and working memory? Prog Brain Res 169, 323–338.

Crosson, B., Sadek, J.R., Maron, L., Gökçay, D., Mohr, C.M., Auerbach, E.J., Freeman, a J., Leonard, C.M., Briggs, R.W., 2001. Relative shift in activity from medial to lateral frontal cortex during internally versus externally guided word generation. J Cogn Neurosci 13, 272–83.

Cunillera, T., Càmara, E., Toro, J.M., Marco-Pallares, J., Sebastián-Galles, N., Ortiz, H., Pujol, J., Rodriguez-Fornells, A., 2009. Time course and functional neuroanatomy of speech segmentation in adults. Neuroimage 48, 541–53.

De Diego-Balaguer, R., Couette, M., Dolbeau, G., Dürr, a, Youssov, K., Bachoud-Lévi, a-C., 2008. Striatal degeneration impairs language learning: evidence from Huntington's disease. Brain 131, 2870–81.

De Diego-Balaguer, R., Lopez-Barroso, D., 2010. Cognitive and Neural Mechanisms Sustaining Rule Learning From Speech. Language Learning 60, 151–187.

De Diego-Balaguer, R., Toro, J.M., Rodriguez-Fornells, A., Bachoud-Lévi, A.-C., 2007. Different neurophysiological mechanisms underlying word and rule extraction from speech. PLoS One 2, e1175.

Doeller, C.F., Opitz, B., Krick, C.M., Mecklinger, A., Reith, W., 2006. Differential hippocampal and prefrontal-striatal contributions to instance-based and rule-based learning. Neuroimage 31, 1802–16.

Dutoit, T., Pagel, V., Pierret, N., Bataille, F., Vrecken, O., 1996. The MBROLA project: Towards a Set of High Quality Speech Synthesizers Free of Use for Non Commercial Purposes., in: Proceedings of ICSLP.

Eichele, T., Debener, S., Calhoun, V.D., Specht, K., Engel, A.K., Hugdahl, K., von Cramon, D.Y., Ullsperger, M., 2008. Prediction of human errors by maladaptive changes in event-related brain networks. Proc Natl Acad Sci U S A 105, 6173–8.

Forn, C., Ripollés, P., Cruz-Gomez, A.J., Belenguer, A., Gonzalez-Torre, J.A., Avila, C., 2013. Task-load manipulation in the Symbol Digit Modalities Test: an alternative measure of information processing speed. Brain Cogn 82, 152–160.

Friston, K.J., 2011. Functional and effective connectivity: a review. Brain connectivity 1, 13–36.

Golestani, N., Pallier, C., 2007. Anatomical correlates of foreign speech sound production. Cereb Cortex 17, 929–34.

Hickok, G., Houde, J., Rong, F., 2011. Sensorimotor integration in speech processing: computational basis and neural organization. Neuron 69, 407–22.

Hickok, G., Poeppel, D., 2000. Towards a functional neuroanatomy of speech perception. Trends Cogn Sci 4, 131–138.

Hickok, G., Poeppel, D., 2007. The corticall organization of speech processing. Nat Rev Neurosci 8, 393–402.

Hikosaka, O., Sakai, K., Miyauchi, S., Takino, R., Sasaki, Y., Pütz, B., 1996. Activation of human presupplementary motor area in learning of sequential procedures: a functional MRI study. J Neurophysiol 76, 617–21.

Jacquemot, C., Scott, S.K., 2006. What is the relationship between phonological short-term memory and speech processing? Trends Cogn Sci 10, 480–486.

Karuza, E.A., Newport, E.L., Aslin, R.N., Starling, S.J., Tivarus, M.E., Bavelier, D., 2013. The neural correlates of statistical learning in a word segmentation task : An fMRI study. Brain & Language.

Koechlin, E., Jubault, T., 2006. Broca's area and the hierarchical organization of human behavior. Neuron 50, 963–74.

Krainik, A., Duffau, H., Capelle, L., Cornu, P., Boch, A., Mangin, J., Le Bihan, D., Marsault, C., Chiras, J., Lehérici, S., 2004. Role of the healthy hemisphere in recovery after resection of the supplementary motor area. Neurology 62, 1323–1332.

Kuperberg, G.R., Holcomb, P.J., Sitnikova, T., Greve, D., Dale, A.M., Caplan, D., 2003. Distinct patterns of neural modulation during the processing of conceptual and syntactic anomalies. J Cogn Neurosci 15, 272–93.

Lambon Ralph, M.A., Ehsan, S., Baker, G.A., Rogers, T.T., 2012. Semantic memory is impaired in patients with unilateral anterior temporal lobe resection for temporal lobe epilepsy. Brain 135, 242–58.

Lau, H.C., Rogers, R.D., Haggard, P., Passingham, R.E., 2004. Attention to intention. Science 303, 1208–10.

Leaver, A.M., Rauschecker, J.P., 2010. Cortical representation of natural complex sounds: effects of acoustic features and auditory object category. J Neurosci 30, 7604–12.

Leh, S.E., Ptito, A., Chakravarty, M.M., Strafella, A.P., 2007. Fronto-striatal connections in the human brain: a probabilistic diffusion tractography study. Neurosci Lett 419, 113–8.

Liberman, A.M., Whalen, D.H., 2000. On the relation of speech to language. Trends Cogn Sci 4, 187–196.

Lieberman, M.D., Cunningham, W.A., 2009. Type I and Type II error concerns in fMRI research: re-balancing the scale. Soc. Cogn. Affect. Neurosci. 4, 423–428.

Lieberman, P., 2000. Human language and our reptilian brain: The subcortical bases of speech, syntax and though, MA: Harvar. ed. Cambridge.

López-Barroso, D., Catani, M., Ripollés, P., Dell'Acqua, F., Rodríguez-Fornells, A., De Diego-Balaguer, R., 2013. Word learning is mediated by the left arcuate fasciculus. Proc Natl Acad Sci U S A 110, 13168–13173.

López-Barroso, D., De Diego-Balaguer, R., Cunillera, T., Camara, E., Münte, T.F., Rodríguez-Fornells, A., 2011. Language learning under working memory constraints correlates with microstructural differences in the ventral language pathway. Cereb Cortex 21, 2742–2750.

MacMillan, N., Creelman, C., 2005. Detection Theory: A User's Guide., Second Edi. ed. Lawrence Elbaum Associated, Publishers.

McKeown, M.J., Jung, T.P., Makeig, S., Brown, G., Kindermann, S.S., Lee, T.W., Sejnowski, T.J., 1998. Spatially independent activity patterns in functional MRI data during the stroop color-naming task. Proceedings of the National Academy of Sciences 95, 803–810.

McNealy, K., Mazziotta, J.C., Dapretto, M., 2006. Cracking the language code: neural mechanisms underlying speech parsing. J Neurosci 26, 7629–7639.

McNealy, K., Mazziotta, J.C., Dapretto, M., 2011. Age and experience shape developmental changes in the neural basis of language-related learning. Dev Sci 14, 1261–82.

Mechelli, A., Crinion, J., Noppeney, U., O'Doherty, J., Ashburner, J., Frackowiak, R., CJ, P., 2004. Structural Plasticity in the biligual brain. Nature 431, 757.

Meister, I.G., Wilson, S.M., Deblieck, C., Wu, A.D., Iacoboni, M., 2007. The essential role of premotor cortex in speech perception. Curr Biol 17, 1692–6.

Mestres-Missé, A., Càmara, E., Rodríguez-Fornells, A., Rotte, M., Münte, T.F., 2008. Functional neuroanatomy of meaning acquisition from context. J Cogn Neurosci 2153–2166.

Mesulam, M.M., 1990. Large-scale neurocognitive networks and distributed processing for attention, language, and memory. Ann Neurol 28, 597–613.

Patterson, K., Nestor, P., Rogers, T., 2007. Where do you know what you know? The representation of semantic knowledge in the human brain. Nat Rev Neurosci 8, 976–987.

Penhune, V.B., Steele, C.J., 2012. Parallel contributions of cerebellar, striatal and M1 mechanisms to motor sequence learning. Behav Brain Res 226, 579–91.

Peña, M., Bonatti, L.L., Nespor, M., Mehler, J., 2002. Signal-Driven Computations in Speech Processing. Science (80-) 298, 604–607.

Pulvermüller, F., Huss, M., Kherif, F., Moscoso del Prado Martin, F., Hauk, O., Shtyrov, Y., 2006. Motor cortex maps articulatory features of speech sounds. Proc Natl Acad Sci U S A 103, 7865–70.

Raichle, M.E., MacLeod, a M., Snyder, a Z., Powers, W.J., Gusnard, D. a, Shulman, G.L., 2001. A default mode of brain function. Proc Natl Acad Sci U S A 98, 676–82.

Rauschecker, J.P., Scott, S.K., 2009. Maps and streams in the auditory cortex: nonhuman primates illuminate human speech processing. Nat Neurosci 12, 718–24.

Ravizza, S.M., Delgado, M.R., Chein, J.M., Becker, J.T., Fiez, J.A., 2004. Functional dissociations within the inferior parietal cortex in verbal working memory. Neuroimage 22, 562–573.

Rodriguez-Fornells, A., Cunillera, T., Mestres-Missé, A., De Diego-Balaguer, R., 2009. Neurophysiological mechanisms involved in language learning in adults. Philos Trans R Soc Lond B Biol Sci 364, 3711–3735.

Saffran, J.R., 2001. Words in a sea of sounds : the output of infant statistical learning. Cognition 81, 149–169.

Saffran, J.R., Aslin, R., Newport, E., 1996. Statistical learning by 8-month-old infants. Science (80-) 274, 1926–1928.

Salmi, J., Rinne, T., Koistinen, S., Salonen, O., Alho, K., 2009. Brain networks of bottom-up triggered and top-down controlled shifting of auditory attention. Brain Res 1286, 155–164.

Saur, D., Kreher, B.W., Schnell, S., Kümmerer, D., Kellmeyer, P., Vry, M.-S., Umarova, R., Musso, M., Glauche, V., Abel, S., Huber, W., Rijntjes, M., Hennig, J., Weiller, C., 2008. Ventral and dorsal pathways for language. Proc Natl Acad Sci U S A 105, 18035–18040.

Saur, D., Schelter, B., Schnell, S., Kratochvil, D., Küpper, H., Kellmeyer, P., Kümmerer, D., Klöppel, S., Glauche, V., Lange, R., Mader, W., Feess, D., Timmer, J., Weiller, C., 2010. Combining functional and anatomical connectivity reveals brain networks for auditory language comprehension. Neuroimage 49, 3187–97.

Smith, S.M., 2012. The future of FMRI connectivity. Neuroimage 62, 1257–66.

Smith, S.M., Fox, P.T., Miller, K.L., Glahn, D.C., Fox, P.M., Mackay, C.E., Filippini, N., Watkins, K.E., Toro, R., Laird, A.R., Beckmann, C.F., 2009. Correspondence of the brain's functional architecture during activation and rest. Proc Natl Acad Sci U S A 106, 13040–5.

Tie, Y., Whalen, S., Suarez, R.O., Golby, A.J., 2008. Group independent component analysis of language fMRI from word generation tasks. Neuroimage 42, 1214–25.

Wilson, S.M., Iacoboni, M., 2006. Neural responses to non-native phonemes varying in producibility: evidence for the sensorimotor nature of speech perception. Neuroimage 33, 316–25.

Wu, X., Lu, J., Chen, K., Long, Z., Wang, X., Shu, H., Li, K., Liu, Y., Yao, L., 2009. Multiple neural networks supporting a semantic task: an fMRI study using independent component analysis. Neuroimage 45, 1347–58.

Xu, J., Potenza, M.N., Calhoun, V.D., 2013a. Spatial ICA reveals functional activity hidden from traditional fMRI GLM-based analyses. Front Neurosci 7.

Xu, J., Zhang, S., Calhoun, V.D., Monterrosso, J., Li, C.S., Worhunsky, P.D., Stevens, M., Pearlson, G.D., Potenza, M.N., 2013b. Task-related concurrent but opposite modulations of overlapping functional networks as revealed by spatial ICA. Neuroimage 79, 62–72.

Zatorre, R.J., Bouffard, M., Belin, P., 2004. Sensitivity to auditory object features in human temporal neocortex. J Neurosci 24, 3637–42.

Ziegler, W., Kilian, B., Deger, K., 1997. The role of the left mesial frontal cortex in fluent speech: evidence from a case of left supplementary motor area hemorrhage. Neuropsychologia 35, 1197–208.

TABLES

Table 1. Different task-related ICA networks with their respective areas of activation and their statistical level of task relatedness for the main experiment in this study (First cohort, n = 27). TRN: task-related network; BA: Brodmann areas; dAPMN: dorsal Auditory-Premotor Network; dSMN: dorsal Sensory-Motor Network; dFPN: dorsal Fronto-Parietal Network; vFTN: ventral Fronto-Temporal Network; DMN: Default Mode Network. * Survived the correction for multiple comparisons.

TRN	Activation Region	BA	Task relatedness *T*-val(*P*-val)
dAPMN Fig. 2A	Bilateral sup/mid temporal gyrus; Bilateral Heschl gyrus; Bilateral insula; Bilateral precentral gyrus; Left postcentral gyrus; Supplementary motor area; Pre-Supplementary motor area	22,21,13,41, 42,6,4	15.20 (0.001)*
dSMN Fig. 2B	Bilateral precentral gyrus; Bilateral postcentral gyrus; Supplementary motor area; Pre-Supplementary motor area; Bilateral middle cingulate gyrus	4,3,6,2,24	3.77 (0.001)*
dFPN Fig. 2C	Left sup/ inf temporal gyrus; Bilateral middle temporal gyrus; Bilateral angular gyrus; Left supramarginal gyrus; Bilateral superior occipital gyrus; Left inf/mid occipital gyrus; Bilateral inf/sup parietal gyrus; Left precuneus; Bilateral inferior frontal gyrus orb/trian/oper; Bilateral middle frontal gyrus; Left superior frontal gyrus; Supplementary motor area; Bilateral precentral gyrus	44,45,46,47, 21,22,20,19, 37,39,40,7, 89,10,11,6	2.12 (0.043)
vFTN Fig. 2D	Bilateral insula; Bilateral temporal pole; Bilateral inf. frontal gyrus pars triang/oper/orb; Bilateral anterior cingulate gyrus; Bilateral frontal superior medial gyrus; Bilateral caudate head; Left globus pallidum; Bilateral mid/sup temporal gyrus; Bilateral supramarginal gyrus; Bilateral angular gyrus; Bilateral inferior parietal gyrus	47,45,44,38, 22,13,40,10, 9,32	2.03 (0.052)
DMN Fig. 3A	Bilateral cuneus; Bilateral precuneus; Bilateral middle occipital gyrus; Bilateral inferior parietal gyrus; Bilateral angular gyrus; Bilateral middle temporal; Bilateral ant/post/mid cingulate gyrus; Bilateral sup/mid frontal gyrus;	40,39,7,22,1 9,31,29,5,23 8,9,10,11,32	-2.58 (0.015)

Table 2. Different task-related ICA networks with their respective areas of activation and their statistical level of task relatedness from the second cohort of subjects (n = 16). TRN: task-related network; BA: Brodmann areas; dAPMN: dorsal Auditory-Premotor Network; dSMN: dorsal Sensory-Motor Network; dFPN: dorsal Fronto-Parietal Network; vFTN: ventral Fronto-Temporal Network; DMN: Default Mode Network; VLN: Visual Lateral Network; IN: Insular Network. * Survived the correction for multiple comparisons.

			Task relatedness
TRN	**Activation Region**	**BA**	*T*-val(*P*-val)
dAPMN Fig. 2A	Bilateral sup/mid temporal gyri; Bilateral Heschl gyri; Bilateral insula; Left precentral gyrus; Left postcentral gyrus;	22,21,13,41,42 6,4	18.00 (0.001)*
dSMN Fig. 2B	Bilateral precentral gyri; Bilateral postcentral gyri; Supplementary motor area; Pre-Supplementary motor area; Bilateral middle cingulate gyri; Bilateral thalamus; Bilateral caudate;	4,3,6,2,24	4.73 (0.001)*
dFPN Fig. 2C	Left inf/mid temporal gyrus; Bilateral angular gyri; Left supramarginal gyrus; Bilateral superior occipital gyri; Left inf/mid occipital gyrus; Bilateral inf/sup parietal gyri; Left precuneus; Left inferior frontal gyrus orb/trian/oper; Bilateral middle frontal gyri; Left superior frontal gyrus; Supplementary motor area; Left precentral gyri; Left Hippocampus;	44,45,46,47,21,22,20,1937,39,40,7,8,9 10,11,6	3.30 (0.004)
vFTN Fig. 2D	Bilateral insula; Bilateral temporal pole; Bilateral inf. frontal gyri pars trian/oper/orb; Supplementary motor area; Bilateral frontal superior medial gyri; Bilateral caudate head; Bilateral globus pallidum; Bilateral middle/superior temporal gyri; Bilateral supramarginal gyri; Bilateral angular gyri;	47,45,44,38 22,21,13,40,89	2.19 (0.045)
DMN Fig. 3B	Bilateral cuneus; Bilateral precuneus; Bilateral superior/middle occipital gyrus; Bilateral anterior/posterior/middle cingulate gyrus; Bilateral angular gyrus; Bilateral sup/infr parietal gyrus; Right middle temporal;	7,31,23,32,40 19,39	-3.13 (0.007)
VLN Fig. S1A	Bilateral mid./sup./inf. occipital gyri; Bilateral sup/inf. parietal gyri; Bilateral fusiform gyri; Bilateral mid/inf temporal; Bilateral postcentral gyri; Bilateral cuneus; Bilateral lingual gyrus; Bilateral Middle Frontal	19,18,7,37,40 10	2.31 (0.035)
IN Fig. S1B	Bilateral insula; Bilateral precentral gyri; Bilateral postcentral gyri; Supplementary motor area; Cuneus;	6,31,13	3.95 (0.0015)*

Table 3. Different non-task-related networks with their respective areas of activation and their statistical level of task relatedness for the first cohort of subjects. NTRN: Non-Task-Related Network; BA: Brodmann areas.

NTRN	**Activation Region**	**BA**	**Task relatedness** *T*-val (*P*-value)
Sup. Parietal	Bilateral precuneus; Bilateral sup/inf parietal gyrus; Bilateral postcentral gyrus; Bilateral middle occipital gyrus; Bilateral middle cingulum;	7,40,5,31	-0.36 (0.71)
Visual Lat.	Bilateral sup/mid/inf occipital gyrus; Bilateral fusiform gyrus; Bilateral mid/inf temporal gyrus; Bilateral lingual gyrus;	19,18,37,7	1.03 (0.31)
Cerebellar	Cerebellum; Vermis; Pons;	-	0.87 (0.39)
Medial Visual	Bilateral calcarine; Bilareal lingual gyrus; Bilateral cuneus; Bilateral middle/superior occipital gyrus; Bilateral precuneus;	19,18,7,31,17 30	-1.12 (0.27)
Cingulate	Bilateral frontal medial gyrus pars orbitalis; Bilateral frontal superior medial gyrus; Bilateral anterior cingulate gyrus; Bilateral rectus; Bilateral caudate;	10,11,32	-0.73 (0.47)
Mesial Temp	Bilateral temporal pole; Bilateral parahipocampal gyrus; Left middle temporal gyrus; Bilateral hippocampus; Bilateral fusiform gyrus; Bilateral amygdala;	38,34,21,28 35,20,28	-0.01 (0.99)
Right Fronto Parietal	Bilateral middle frontal gyrus; Right superior frontal gyrus; Right inferior frontal gyrus part orb/trian/oper; Right frontal medial gyrus pars orbitalis; Right frontal superior medial gyrus; Right precentral gyrus; Right anterior cingulate gyrus; Bilateral middle cingulate gyrus; Bilateral angular gyrus; Bilateral superior/inferior parietal gyrus; Bilateral precuneus; Right supramarginal gyrus; Right mid/sup occipital gyrus;	10,9,8,6,46 11,47,45,4 32,23,40,7 39	1.20 (0.23)

Table 4. Different non-task related networks with their respective areas of activation and their statistical level of task relatedness for the second cohort of subjects. NTRN: Non-Task-Related Network; BA: Brodmann area

NTRN	**Activation Region**	**BA**	**Task relatedness** *T*-val (*P*-val)
Med. Inf. Visual	Bilateral Calcarine; Bilateral inf/mid occipital gyrus;	18,17	-0.38 (0.70)
Cerebellar	Cerebellum; Vermis; Pons	-	-1.93 (0.07)
Medial Visual	Bilateral calcarine; Bilareal lingual gyrus; Bilateral cuneus; Bilateral mid/sup occipital gyrus; Bilateral precuneus	19,18,7,31,17 30	-1.47 (0.16)
Posterior DMN	Bilateral frontal medial gyrus pars orbitalis; Bilateral frontal superior medial gyrus; Bilateral anterior cingulate gyrus; Bilateral rectus; Bilateral caudate; Bilateral precuneus; Bilateral posterior cingulate gyrus;	10,11,32,31	0.10 (0.92)
Mesial Temporal	Bilateral temporal pole; Bilateral parahipocampal gyrus; Bilateral mid/inf temporal gyrus; Bilateral hippocampus; Bilateral fusiform gyrus; Bilateral amygdala;	38,34,21,28 35,20,28	1.78 (0.095)
Right Fronto Parietal	Right mid/sup frontal gyrus; Right inferior frontal gyrus part orb/trian/operc; Right frontal superior medial gyrus; Bilateral angular gyrus; Right supramarginal gyrus; Bilateral sup/inf parietal gyrus; Right postcentral gyrus;	10,8,9,6,46,45 47,11,40,7,39	-1.46 (0.16)
Superior Medial Fronto-Parietal	Bilateral frontal superior medial gyrus; Bilateral superior middle/frontal gyrus; Bilateral anterior cingulate gyrus; Bilateral angular; Left supramarginal gyrus; Bilateral inferior parietal gyrus	10,8,9,6,40,39	-1.05 (0.30)

Table 5. Statistical indexes of task relatedness for each of the four blocks that composed the word learning task. TRN: task-related network; BA: Brodmann areas; dAPMN: dorsal Auditory-Premotor Network; dSMN: dorsal Sensory-Motor Network; dFPN: dorsal Fronto-Parietal Network; vFTN: ventral Fronto-Temporal Network; DMN: Default Mode Network; VLN: Visual Lateral Network; IN: Insular Network. * Survived the correction for multiple comparisons.

Block	TRN	T-value	d.f.	T-value
1	dAPMN	17.6	26	0.001*
	dSMN	4.74	26	0.001*
	dFPN	2.67	26	0.015
	vFPN	2.13	26	0.043
	DMN	-2.85	26	0.009
2	dAPMN	13.43	26	0.001*
	dSMN	0.29	26	0.77
	dFPN	1.57	26	0.12
	vFPN	0.36	26	0.72
	DMN	-2.79	26	0.01
3	dAPMN	18.26	26	0.001*
	dSMN	0.93	26	0.36
	dFPN	1.12	26	0.27
	vFPN	-0.53	26	0.60
	DMN	-1.69	26	0.10
4	dAPMN	15.55	26	0.001*
	dSMN	4.4	26	0.001*
	dFPN	0.84	26	0.40
	vFPN	-0.03	26	0.97
	DMN	-1.44	26	0.16

FIGURES

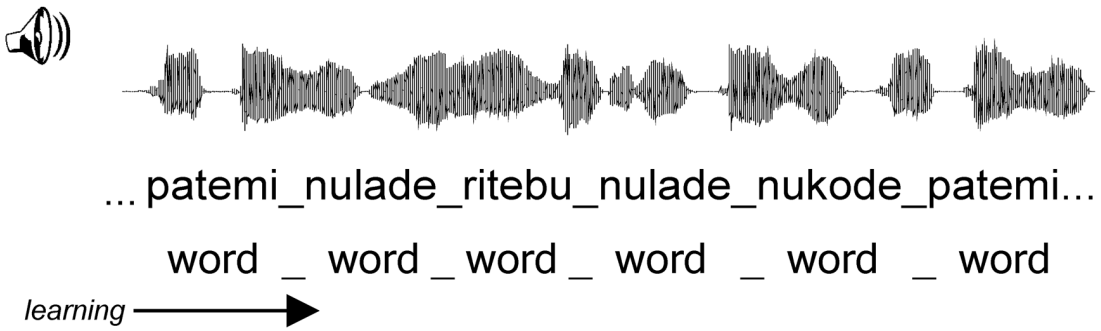

Figure 1. Schematic illustration of the artificial language stream used in the learning phase of the experiments. The stream was aurally presented and it was composed of nonsense trisyllabic words that were repeated across the stream. The "_" represent the 25 millisecond pause inserted between the words in order to mark word boundaries.

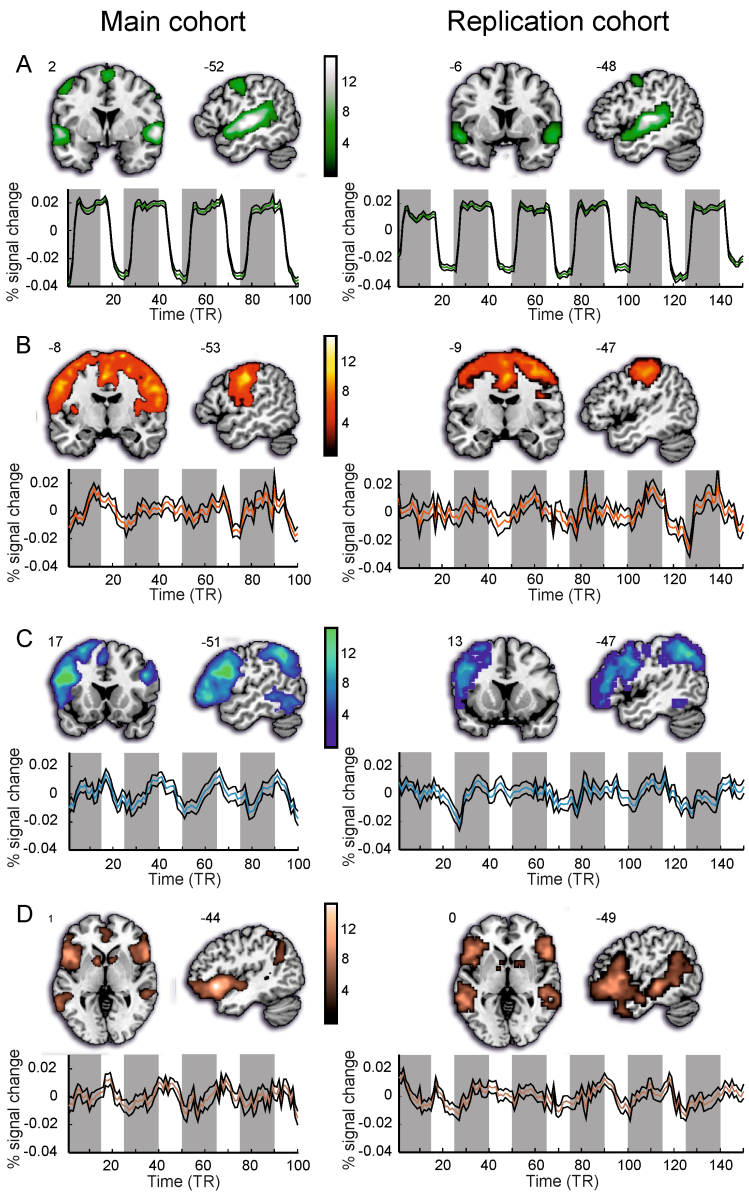

Figure 2. Task-related networks and associated hemodynamic time courses for the first (left panel) and the second (right panel) cohorts. Three of the networks are identified as dorsal networks: *dorsal Auditory-Premotor* (A); *dorsal Sensory-Motor* (B); and *dorsal Fronto-Parietal* (C). The fourth network is identified as a *ventral Fronto-Temporal* (D). Each component is rendered onto the MNI template at representative slices, with MNI coordinates in millimeters shown in the top left corners. Components are shown with a cluster extent of 30 voxels with a 1% false discovery rate with the threshold bar shown at the right side of each panel. On the lower part of each panel, the associated time course for each component is shown. The mean time course over the 27 subjects (first cohort) and the 16 subjects (second cohort) is shown in a central, colored line with standard error of the mean depicted with white lines. Only left hemisphere is shown in the sagittal views. The y-axis represents the percentage of signal change.

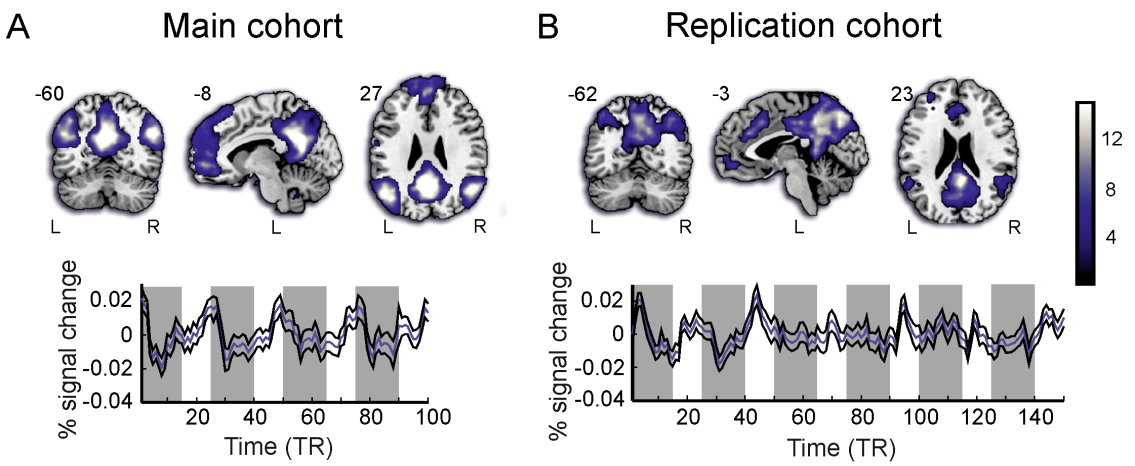

Figure 3. The default mode network, which resulted anticorrelated with the task in the first (A) and the second (B) cohorts, is rendered onto the MNI template at representative coronal, sagittal and axial slices with MNI coordinates in millimeters shown in the top left corners. The average time course over the 27 subjects in the first cohort and the over the 16 subjects in the second cohort (blue line) and the standard error of the mean (white lines) are shown. The components are shown with a cluster extent of 30 voxels with a 1% false discovery rate with the threshold bar shown at the right of the panel. L: left; R: right.

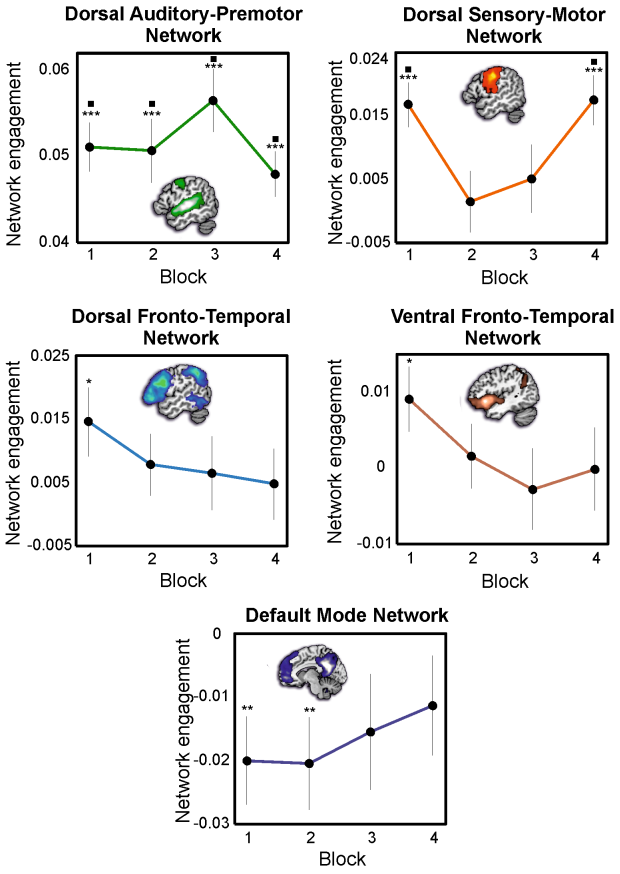

Figure 4. Illustration of the average network engagement for each block and network for the main sample. Bars indicate SEM. * $p < 0.05$; ** $p < 0.01$; *** $p < 0.001$; · survived the correction for multiple comparisons.

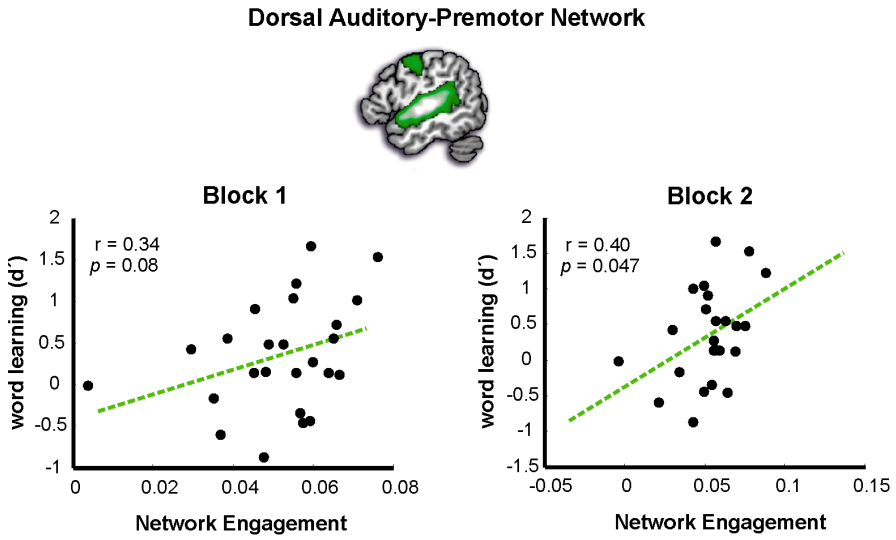

Figure 5. Scatter plots showing the relationship between network engagement and word learning performance in block 1 and block 2 for the dorsal auditory-premotor network. Correlation indexes and the associated p values are depicted on each plot.

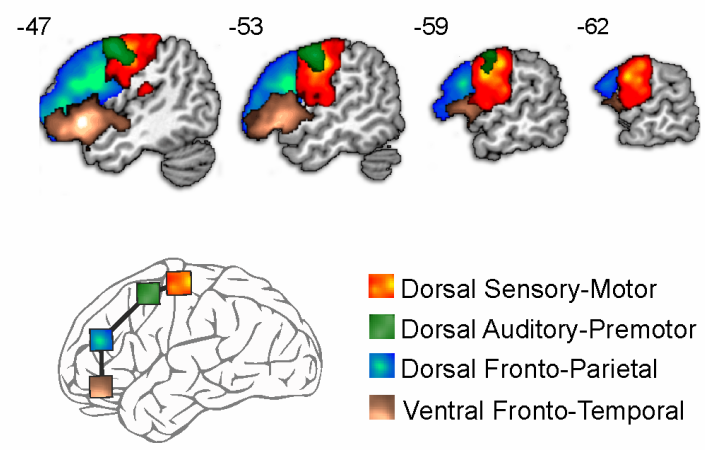

Figure 6. Illustration of the frontal region covered by each of the four networks retrieved in the left hemisphere for the first cohort. For display purposes, only the frontal clusters of each network are shown in this figure. MNI coordinates in millimeters are shown in the top left corners of each slice.